Mine Water and the Environment (2024) 43:658–674
https://doi.org/10.1007/s10230-024-01016-x

TECHNICAL ARTICLE

Microbial Sulfur Pathways and Outcomes in Tailings Impoundments: A Mesocosm Study

Jay Gordon[1] · Simon C. Apte[2] · Tara E. Colenbrander Nelson[1] · Kelly J. Whaley-Martin[1] · Lauren E. Twible[1] · LinXing Chen[3] · Felicia Liu[1] · Samantha McGarry[4] · Jillian F. Banfield[3] · Lesley A. Warren[1]

Received: 26 March 2024 / Accepted: 7 November 2024 / Published online: 28 November 2024

Abstract

In mine wastewaters, three microbial sulfur oxidation pathways have the potential to cause different water quality outcomes. These outcomes can differ from abiotic models of sulfate and acidity predictions currently used to monitor potential sulfur risks. However, studies integrating microbiology and geochemistry in active mine tailings impoundments are very limited. Here, we developed a novel diagnostic approach to detect microbially driven sulfur pathways. Within this 28-day study, eight on-site, 500 L mesocosms were filled with water extracted directly from the water cap of an active Ni/Cu mine tailings impoundment. Diverse combinations of tailings, sulfur compounds, and nitrate amendments were added to the mesocosms simulating common operational variations experienced by active tailings impoundments. Mesocosm results linked complete SOx, S_4I, and incomplete SOx + rDSR pathway occurrence (metagenomes, inferred from the identity, i.e. 16S rRNA) and activity (mRNA) to physiochemistry and sulfur geochemistry. By integrating the three lines of evidence, the diagnostic approach was able to identify which sulfur pathways were active under varying physiochemical conditions and how geochemical outcomes were affected. A relationship emerged between acid generation and *soxCD* expression (*soxCD* expression indicates the complete SOx pathway activity). However, observed proton yields and sulfate concentrations were less than those predicted by complete SOx pathway activity alone. This indicates other sulfur pathways, e.g. the partial S_4I pathway (within *Thiomonas* and *Halothiobacillus*), and/or activity of the incomplete SOx pathway (within *Thiobacillus* and *Desulfurivibrio*) when either not coupled to rDSR, or paired with use of nitrate, influenced overall sulfur outcomes along with the complete SOx pathway.

Keywords Sulfur-oxidizing bacteria (SOB) · Mine wastewater · Acidity · Sulfur oxidation pathways · Canada

Introduction

Wastewaters associated with base metal mining commonly contain higher concentrations of reduced sulfide (HS^-), sulfur oxidation intermediate compounds (SOI, e.g. thiosulfate ($S_2O_3^{2-}$), tetrathionate ($S_4O_6^{2-}$), zero valent sulfur (ZVS; S^0), etc.) and metals than freshwater and marine systems, and consistently contain moderate levels of nitrate (Miettinen et al. 2021; Skousen et al. 2017; Whaley-Martin et al. 2019, 2020). These high sulfur concentrations result from storage of tailings in wastewater impoundments that are managed on site. Wastewater systems are maintained at circumneutral pH values, unlike acid rock drainage (ARD) conditions, where iron metabolizing genera such as *Ferrovum* and *Acidithiobacillus* link sulfur metabolism with iron oxidation in systems where the pH is low (Grettenberger et al. 2020; Wang et al. 2019). The oxidation of sulfur compounds by sulfur oxidizing bacteria (SOB), such as *Halothiobacillus, Thiomonas, Thiobacillus* and *Thiovirga* in circumneutral wastewater, can lead to water quality concerns. The most notable concerns include surface water acidification approaching ARD conditions, oxygen consumption, and metal mobilization (Camacho et al. 2020b;

✉ Lesley A. Warren
lesley.warren@utoronto.ca

1 Civil and Mineral Engineering, University of Toronto, Toronto, ON, Canada

2 CSIRO Environment, Lucas Heights, NSW, Australia

3 Earth and Planetary Sciences Dept, University of California, Berkeley, Berkeley, CA 94720, USA

4 Glencore, Sudbury Integrated Nickel Operation, Sudbury, ON, Canada

Miettinen et al. 2021; Nancucheo et al. 2017; Skousen et al. 2017; Verburg et al. 2009). Across all studied contexts, SOB communities have demonstrated the ability to catalyze sulfur oxidation using three known biochemical pathways, i.e., (1) complete sulfur oxidation (cSOx), (2) tetrathionate intermediate (S_4I), and (3) incomplete sulfur oxidation (iSOx, lacking the sulfur cycling enzyme SoxCD) coupled to reverse dissimilatory sulfate reduction (rDSR, see Table S-1 (Dahl 2005; Wasmund et al. 2017; Watanabe et al. 2019)). Although the gene expression profiles of sulfur pathways have been extensively studied in the deep terrestrial subsurface and deep sea hydrothermal vents, little is known about how geochemical conditions affect the occurrence or activity of sulfur oxidizing pathways in mining contexts (Bell et al. 2020; Cron et al. 2020).

If driven to completion, these three sulfur pathways produce equivalent proton yields, dependent on the terminal electron acceptor (TEA): $\Delta H^+/\Delta S–S_2O_3^{2-} = 1$ with O_2 as a TEA, and $\Delta H^+/\Delta S–S_2O_3^{2-} = 0$ with NO_3^- as a TEA (supplemental Table S-1). However, the inclusion of sub-steps in each pathway introduces complexity to the proton balance. Specifically, the cSOx pathway catalyzes the direct oxidation of $S_2O_3^{2-}$ to SO_4^{2-}, generating acidity (Friedrich et al. 2005):

$$S_2O_3^{2-} + H_2O + 2\,O_2 \rightarrow 2\,SO_4^{2-} + 2\,H^+ \quad (1)$$

In contrast, the S_4I pathway begins with oxidative condensation of thiosulfate to tetrathionate ($S_4O_6^{2-}$) via the enzyme TsdA, or infrequently via DoxDA, resulting in a net decrease in acidity (Beard et al. 2011; Rameez et al. 2020; Zhang et al. 2020):

$$2S_2O_3^{2-} + 2\,H^+ + 1/2\,O_2 \rightarrow S_4O_6^{2-} + H_2O \quad (2)$$

The subsequent processing of tetrathionate is highly debated, indicating a knowledge gap, and this processing does not necessarily occur immediately following its production (Dam et al. 2007; Kappler et al. 2001; Rameez et al. 2020; Wei et al. 2023). Some studies suggest that the second stage of the S_4I pathway (catalyzed by TetH, and/or other enzymes) results in intracellular ZVS storage (Kanao et al. 2007; Meulenberg et al. 1992b), which delays the release of additional protons yielded by its oxidation (for the potential role of other S_4I pathway enzymes, see Table S-1). Finally, the iSOx + rDSR pathway oxidizes $S_2O_3^{2-}$ to SO_4^{2-}, via several reaction steps. This begins with pH-neutral $S_2O_3^{2-}$ hydrolysis and intracellular storage of ZVS via the iSOx pathway:

$$S_2O_3^{2-} + 1/2\,O_2 \rightarrow SO_4^{2-} + S^0(\text{attached to SoxYZ}) \quad (3)$$

This ZVS is thought to represent a dynamic sulfur sink, oxidized only when other aqueous sulfur substrates are scarce (Hensen et al. 2006), suggesting that the acidity produced by the subsequent rDSR pathway would also be delayed (Table S-1). ZVS and other SOI compounds may also be processed through metabolic pathways that have yet to be identified.

In summary, proton yield can be affected by both the reactions involved in sulfur oxidation through each of the three sulfur pathways presented here, as well as TEA pairing with either oxygen or nitrate. Recently Whaley-Martin et al. (2023) identified differential sulfur oxidation pathway expression based on O_2 and NO_3^- concentrations. In that study, cSOx pathway abundance and activity was linked to oxygen availability (*Halothiobacillus* and *Thiomonas*), while the iSOx + rDSR pathway (*Thiobacillus*) dominated under anoxic conditions in a tailings impoundment's summer stratified water column. Under low pH conditions, these systems move into a state where iron becomes an important e^- donor or acceptor, but iron does not play a major role at circumneutral pH when nitrate is available (Grettenberger et al. 2020; Jin and Kirk 2018; Warren et al. 2008).

The objective of this study was to explore how the occurrence and activity of cSOx, S_4I, and iSOx + rDSR pathways varied in response to available TEAs (O_2, and NO_3^-), sulfur substrates ($S_2O_3^{2-}$ and $S_4O_6^{2-}$), and tailings additions under ambient environmental conditions experienced by an active tailings impoundment. Field-based mesocosm experiments offered the opportunity to mimic the water cap of a tailings impoundment system by using wastewaters drawn directly from the adjacent tailings impoundment under site conditions, at a greater scale than laboratory microcosms allow. Geochemical and biological responses were measured under experimental amendments of (1) tailings, (2) thiosulfate, or (3) tetrathionate, with or without (4) nitrate. Over the course of 28 days, these mesocosms were examined through complementary methods measuring bacterial community composition (16S rRNA gene sequences), functional repertoires (metagenomes), gene expression (mRNA), sulfur compounds ($S_2O_3^{2-}$, $S_4O_6^{2-}$, S^0, SO_4^{2-}), N species (NO_3^-, NO_2^-, NH_4^+), as well as oxygen concentrations and pH; samples for these parameters were collected at different frequencies. A new diagnostic approach was then developed that combines these three lines of evidence (geochemical, community composition linked to functional repertoires, and gene expression), to generate a more holistic understanding of microbial sulfur oxidation and outcomes in this mine tailings impoundment. Through this approach, parallel sulfur pathway activation and terminal electron acceptor switching (from oxygen to nitrate) were discernible.

Methods

Detailed methods for location, mesocosm set-up, and experimental pre-conditioning are described in the supplemental information.

Experimental Phase

On September 22nd, 2020, the eight experimental mesocosms filled with ≈ 470 L of tailings wastewater on July 23rd, 2020, were sampled at day_0 (mesocosms experienced varied pre-conditioning amendments and thus varied microbial communities associated with eight weeks of possible community succession), to characterize initial communities and geochemical conditions ahead of additional experimental manipulation (Fig. 1). All mesocosms were then treated with varying combinations of 12 L tailings, a mix of equal volumes of low sulfur mill waste and pyrrhotite tailings (T_{12}), 2.0 mM S sulfur substrate ($K_2S_4O_6$: $S_{4(2.0)}$ or $Na_2S_2O_3$: $S_{2(2.0)}$), and 2.0 mM nitrate ($NaNO_3$: $N_{2.0}$) amendments creating eight unique experimental treatments outlined in Table 1 and Fig. 1b.

Mesocosms E_1–E_4, E_7, and E_8 received tailings amendments as a mechanism for decreasing oxygen concentrations through oxidative processes to investigate possible hypoxic-anoxic condition impacts on SOB communities, S oxidizing pathway activity, and acidity generation. Data loggers were deployed at the initiation of the experiment (at depths of 20 cm and 50 cm in each mesocosm) to monitor dissolved oxygen concentrations (HOBO® U26-001), and pH (HOBO® MX2501) in each mesocosm. The loggers, initiated at day_0, collected data at 30 min intervals over the 28 days of the experiment.

Prior to the experimental phase, mesocosms were preconditioned with tailing and/or thiosulfate treatments (Fig. 1) and remained at pH 4 but returned to circumneutral following tailings amendments made at day_0. The composition of tailings from the mine have previously been characterised and reported (Duffy et al. 2015). The nickel-rich tailings are composed primarily of pyrrhotite (60%) with associated silica gangue phases (e.g. quartz and albite) comprising around 30% of total mass. Minor mineral components include chalcopyrite, pentlandite and magnetite.

Total alkalinity measurements (Lipps et al. 2023) indicated mean total alkalinity values of 530 mg $CaCO_3$/L, or 10.6 meq/L for the undiluted mine tailings slurry. Note that total alkalinity also includes protonation reactions involving mineral phases as well as carbonate equilibria. Alkalinity measurements from the waters of the mesocosms were negligible throughout the experiment (< LOD by day_3).

Thus, the experiments here explored the effects of $S_2O_3^{2-}$, $S_4O_6^{2-}$, as well as O_2 and NO_3^- concentrations (E_1–E_8, Fig. 1b) on sulfur metabolizing microbial community composition, abundance, and presence/activity of S oxidation pathways (cSOx, iSOx + rDSR, and S_4I) of SOB communities presumed to be differentiated, driven by varied preconditioning amendments. Tailings impoundments are dynamically exposed to operational changes in tailings discharges in addition to seasonal and spatial biogeochemical and environmental variability, the experiments here provide new insights into how communities may change in response to such geochemical and physicochemical changes, and in turn, influence water chemistry outcomes.

Geochemistry

Detailed methods for geochemical analyses are described in Whaley-Martin et al. (2019), and in the supplemental information of this document. Briefly, dissolved $S_4O_6^{2-}$, SO_4^{2-}, NO_2^-, NO_3^-, and NH_4^+ concentrations were determined for triplicate filtered (0.2 µm) samples, on an Thermo Scientific Dionex™ ICS-6000 ion chromograph (IC) system with anion and cation columns (a Dionex IonPac™ AS18-FAS-TAS18 anion exchange, Dionex IonPac™ AS32-Fast-4 µm, and Shodex IC YS-50 columns).

Quantification of $S_2O_3^{2-}$ and SO_3^{2-} (monobromobimane derivatives) was performed in triplicate by high performance liquid chromatography (HPLC) Prominence, Shimadzu system, with an Alltima™ HP C18 reversed phase column. Total S detection was performed in triplicate on 0.2 um and UF samples using an inductively coupled plasma—optical emission spectrograph (ICP-OES, iCAP 7000 Series, Thermo Scientific™) with radial emission from wavelength 180.731 selected for standard curve calibration.

Genomics and Data Analysis

DNA and RNA were extracted with DNeasy PowerWater DNA Isolation and RNeasy PowerWater QIAGEN kits, sequenced using Illumina at the McMaster University Genomics Facility, and Illumina transcriptomic data reads were assembled using gene mapping at Berkeley (using BBTools, Prodigal, Bowtie2, and samtools, see supplemental information for details). Statistical analyses were performed in Excel and RStudio (R version 3.6.2, using Vegan, complex heatmap, and Ggbreak packages). See the methods provided in the supplemental information for details.

Results: Mesocosm Study

In the mesocosm study, mine water taken from the tailings impoundment was exposed to different experimental amendments of NO_3^- (a compound often found in mine

(a)

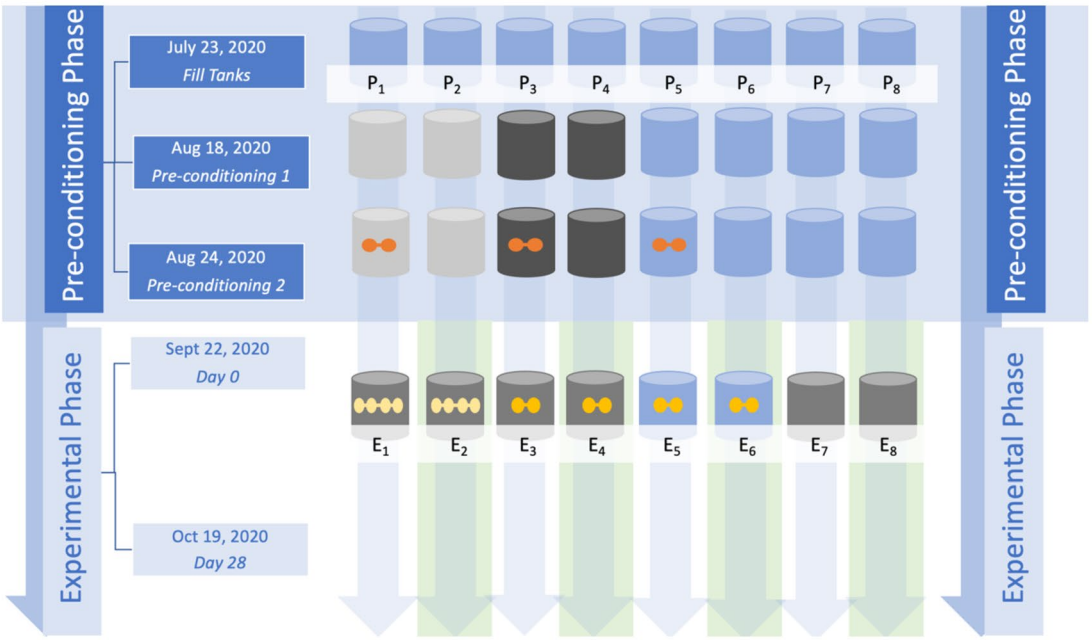

MESOCOSM LEGEND

P_x = Pre-conditioning Phase (Mesocosm #)

Water was initially filled to 100 cm depth. During the preconditioning phase ~136 L were removed, so that by the beginning of experimental phase the water level was at 70 cm depth, and 330 L remained.

E_x = Experimental Phase (Mesocosm #)

Tailings Amendments	Sulfur Amendments	Nitrate Amendments
6.8 L Tailings	2.6 mM $S\text{-}S_2O_3^{2-}$ (as $Na_2S_2O_3$)	2.0 mM NO_3^- (as $NaNO_3$)
13.6 L Tailings	2.0 mM $S\text{-}S_2O_3^{2-}$ (as $Na_2S_2O_3$)	
12 L Tailings	2.0 mM $S\text{-}S_4O_6^{2-}$ (as $K_2S_4O_6$)	

Sample collection timeline (right).
Sample collected from 50 cm depth.
(See Table 1 for list of treatments by mesocosm.)

Date	Day	Geochem	DNA	RNA
Sept 22	0	o	o	o
Sept 23	1.25	o		
Sept 24	2	o		o
Sept 25	3	o		o
Oct 7	16	o	o	
Oct 19	28	o	o	o

(b)

◂**Fig. 1** Field study design. **a** The 500 L mesocosms were embedded in the ground and filled onsite with tailings impoundment wastewater in late July, 2020, and preconditioned prior to experimentation. **b** At day_0 (September 22nd, 2020), several sulfur, nitrate and tailings amendments were added to the mesocosms for the experimental phase (indicated to the left) and sampled at several timepoints until day_{28} on October 19, 2020 (right)

wastewaters from blasting residues), sulfur substrates ($S_2O_3^{2-}$ and $S_4O_6^{2-}$), and tailings. Over the course of 28 days the mesocosms were sampled for physio-chemistry (pH, $[O_2]$, temperature (°C)), sulfur speciation and concentration, 16S rRNA gene sequencing, and mRNA analyses.

Geochemistry: Alkalinity and Acidity Trends

Over the 28-day experiment, five mesocosms (E_1, E_2, E_3, E_5 and E_8) experienced pH decreases/net acidity generation (supplemental Table S-2). The water contained in mesocosms E_1 and E_2 (tetrathionate and tailings additions with or without nitrate) experienced a pH decrease from 6.5 to 5.2 ($\Delta H^+ = 0.0056$ mM) and 6.2 to 5.6 ($\Delta H^+ = 0.0011$ mM) respectively. Water in mesocosms E_3 and E_5 (thiosulfate or without tailings additions) decreased in pH from 7.4 to 6.1 ($\Delta H^+ = 0.0008$ mM) and 6.1 to 5.8 ($\Delta H^+ = 0.0013$ mM) respectively. Mesocosm E_8 (tailings additions with nitrate) had pH that decreased from 7.0 to 6.0 ($\Delta H^+ = 0.0008$ mM).

Over the same timeframe, the remaining three mesocosms (E_4, E_6, and E_7) experienced pH increases, indicating proton consuming reactions were dominant (Table S-2). Mesocosms E_4 and E_6 (thiosulfate with nitrate, with or without tailings) experienced a pH increase from 5.6 to 6.5 ($\Delta H^+ = -0.0019$ mM), and 4.0 to 7.1 ($\Delta H^+ = -0.0954$ mM), respectively. The least change in proton concentration was observed in the tailings mesocosm, E_7 (tailings), where the pH rose from 6.5 to 6.7 ($\Delta H^+ = -0.0001$ mM).

Acid neutralization calculations that accounted for the alkalinity of the added tailings slurry (530 mg $CaCO_3$/L, or 10.6 meq/L) indicated that following the initial upward pH adjustment, the added tailings alkalinity had only a slight moderating effect on solution pH. The potential effect of the diluted tailings alkalinity on the attenuation acidity generation was assessed by calculation of proton equilibria using a spreadsheet model based on the model of Nhantumbo et al. (2018). As part of the development of the spreadsheet model, test calculations were validated against predictions obtained from the geochemical model PHREEQC. Alkalinity measurements from the waters of the mesocosms were also negligible throughout the experiment (< LOD by day_3). Calculations indicated that the low acid generation observed in the mesocosms could not account for the neutralisation of acid by the small concentration of tailings total alkalinity. For instance, in mesocosm E_3, the decrease in thiosulphate concentration over the duration of the experiment was 0.55 mM. If this concentration of thiosulphate was oxidised via the cSOx pathway, it would be predicted to generate a pH of 2.7 in an unbuffered solution compared to the pH of 2.9 pH observed in the solution containing tailings, or the observed final pH in the experiment of 6.1. Thus, there was a reasonable basis to exclude tailings alkalinity from proton yield calculations. This supports the assumption that net ΔH^+ represents actual acidity produced by microbial processes.

Geochemistry: Sulfur Speciation Trends

Although baseline sulfate concentrations in the wastewater were high (ca. 7.6 mM) prior to the experimental phase, all eight mesocosms showed increases in sulfate over the 28 days (Fig. 2, Table S-2). Mesocosms E_1–E_4 averaged ΔSO_4^{2-} of 1.6 ± 0.3 mM, and mesocosms E_5–E_8 had averaged $\Delta SO_4^{2-} = 0.6 \pm 0.2$. mM. The thiosulfate concentration decreased in all mesocosms, following a pseudo-first order reaction (calculated according to Eq. 4):

$$\left[S_2O_3^{2-}\right] = \left[S_2O_3^{2-}\right]_0 e^{-k't} \quad (4)$$

where t is time, and k' is the first derivative of the rate constant for a first order reaction (Table S-3. This thiosulfate loss indicates processing via any of the three pathways (Eqs. 1–3).

Low concentrations of S^0 (0.01–0.48 mM, $[S^0]_{median} = 0.05$ mM) were detected in all mesocosms over the experiment's duration. The lowest S^0 concentrations were found in tailings-only treatments (E_7 and E_8 Fig. 2, Table S-2), indicating tailings were not a substantial S^0 source.

In the tetrathionate-amended mesocosms, a large tetrathionate loss over the course of the experiment ($\Delta S\text{-}S_4O_6^{2-} = -0.39$ mM) occurred in mesocosm E_1, but not in tetrathionate and nitrate amended E_2 ($\Delta S\text{-}S_4O_6^{2-} = 0.02$ mM). Similarly, a small tetrathionate loss ($\Delta S\text{-}S_4O_6^{2-} = -0.06$ mM) was measured in the thiosulphate amended mesocosm (E_3), but not the thiosulfate and tailings amended E_4 ($\Delta S\text{-}S_4O_6^{2-} = 0.03$ mM). However, these data are only semi-quantitative as the 0.2 µm filtered samples produced a high standard deviation, perhaps because of sampling variation or storage for > 1 year prior to analysis. The detection of tetrathionate concentrations greater than the background level of 0.1 mM also occurred in the tailings-only control mesocosms (E_7 and E_8), and in the thiosulfate amended mesocosms where no tetrathionate was added (E_3–E_6, see Fig. 2, Table S-2).

In most mesocosms, measured sulfur species accounted for over 90% of the total sulfur present (Fig. 2, Table S-2). However, larger gaps in the sulfur mass balance occurred

Table 1 Experimental treatments in 8 mine wastewater 500 L mesocosms

Mesocosm	Tailings amendment	Sulfur substrate amendment	Nitrate amendment	Treatment code
E_1	12 L	2.0 mM S–$S_4O_6^{2-}$	–	$T_{12}S_{4(2.0)}$
E_2	12 L	2.0 mM S–$S_4O_6^{2-}$	2.0 mM NO_3^-	$T_{12}S_{4(2.0)}N_{2.0}$
E_3	12 L	2.0 mM S-$S_2O_3^{2-}$	–	$T_{12}S_{2(2.0)}$
E_4	12 L	2.0 mM S–$S_2O_3^{2-}$	2.0 mM NO_3^-	$T_{12}S_{2(2.0)}N_{2.0}$
E_5	–	2.0 mM S-$S_2O_3^{2-}$	–	$S_{2(2.0)}$
E_6	–	2.0 mM S-$S_2O_3^{2-}$	2.0 mM NO_3^-	$S_{2(2.0)}N_{2.0}$
E_7	12 L	–	–	T_{12}
E_8	12 L	–	2.0 mM NO_3^-	$T_{12}N_{2.0}$

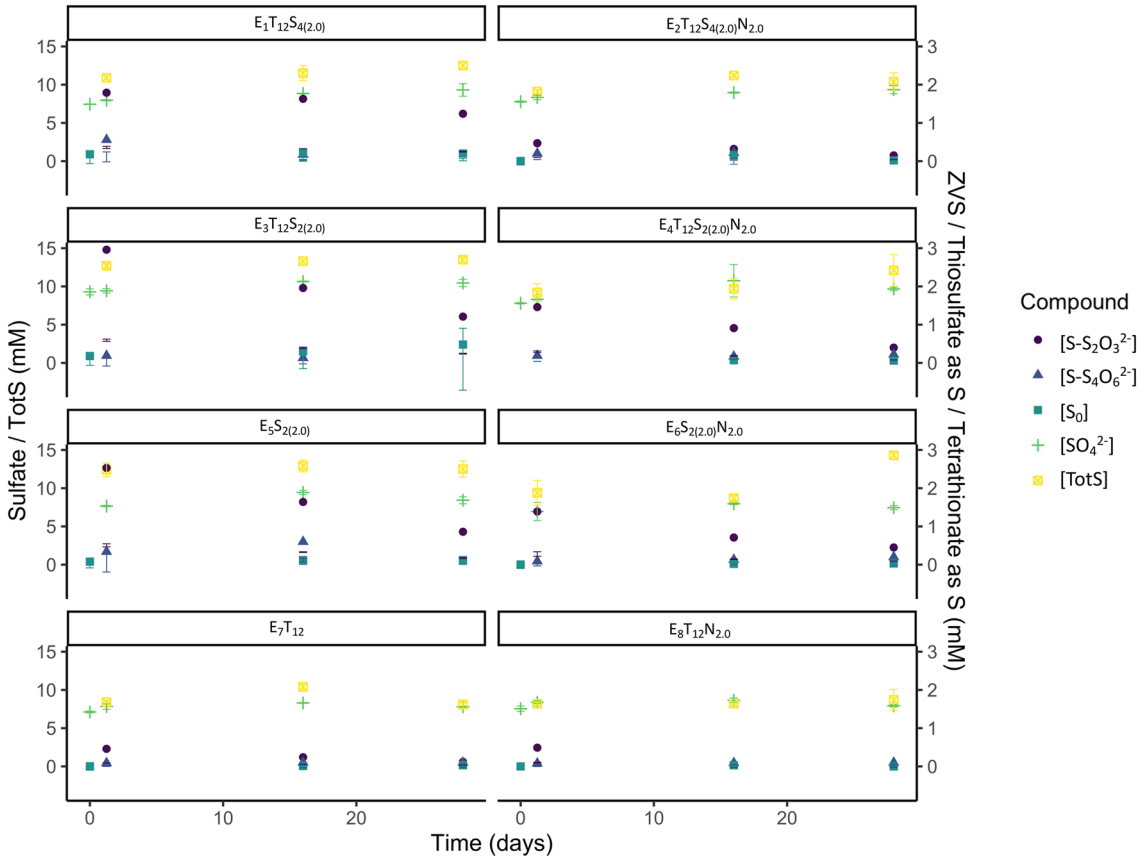

Fig. 2 Changes in sulfur speciation trends across the 8 mesocosms are shown above. Sulfite concentrations, [SO_3^{2-}], were non-detect for all systems and timepoints. (Where standard deviation values for data were not available, the mean values of 0.05 mM for S–$S_4O_6^{2-}$ and 0.1 mM for S^0 are presented.)

at day_{28} (Total S—$\sum$ measured sulfur species) for the two thiosulfate and tailings amended mesocosms, E_5 (75% of TotS) and E_6 (57% of TotS). This indicates the formation of other unidentified SOI species. In mesocosms E_3, E_5, E_7 and E_8, not all thiosulfate loss can be accounted for by increases in sulfate ($\Delta[SO_4^{2-}] < -\Delta[S_2O_3^{2-}]$), also suggesting the formation of SOIs such as polythionates. Alternately, gaps in the S mass balance may be partially accounted for by ZVS formation, and subsequent sedimentation through excretion or cell death.

Geochemistry: Oxygen and Nitrate Availability for Sulfur Compound Oxidation

Published experimental evidence suggests that nitrate and oxygen are used concurrently by SOB below 0.3 mg/L O_2, and that a decrease in use of nitrate occurs above that

threshold O_2 concentration (Wang et al. 2016; Zhang et al. 2019). Therefore, we conservatively estimated 0.5 mg/L (0.016 mM) as the concentration above which oxygen is used exclusively.

Dissolved oxygen concentrations varied with time, depth, and mesocosm (Table S-2; supplemental Fig. S-1). Yet, except for E_6, all mesocosms experienced some periods of oxygen depletion below the assigned threshold value (< 0.016 mM, Table 2), often during the first 10 days. Nitrate was detected at all timepoints (Table S-2) suggesting SOB had the opportunity to use nitrate as an alternate TEA to oxygen. However, the simultaneous increases in nitrate and ammonia observed in all tanks over the experimental period are consistent with activity of both N-reducing and N-oxidizing microorganisms.

Nitrate amendments increased thiosulfate oxidation rates in the mesocosms containing tailings. Thiosulfate oxidation rates increased by 1.7-fold in the tailings plus thiosulfate treatments (E_4 and E_3) when amended with nitrate (the half-life of E_4 13.9 days with nitrate, and of E_3 was 21.3 days without nitrate). This was also observed when comparing tailings only treatment where there was 2.8-fold increase in thiosulfate oxidation with nitrate. (A thiosulphate half-life of 4.95 days was measured with nitrate (E_8), compared to a half-life of 13.9 days without nitrate (E_7); see Table S-3). In addition, nitrate-amended treatments (E_2, E_4, E_6) had lower [S^0] compared to their nitrate-free equivalents, and generally showed a decrease in [S^0] over the latter half of the experiment (Table S-2).

Bacteria: Sulfur Metabolizing Community Trends (16S rRNA)

Six SOB genera (*Halothiobacillus, Thiomonas, Sediminibacterium, Thiovirga, Acidovorax* and *Sulfurovum* and one sulfur reducing bacteria, also able to oxidize sulfur (*Desulfurivibrio*, (Melton et al. 2016; Sun et al. 2022; Thorup et al. 2017)), were identified through 16S rRNA gene expression (Fig. 3b, Table S-4). An additional nitrate-dependent iron oxidizing (NDFO) genus (*Acidovorax*) was found to also have tetrathionate reducing genes (Fig. 3b, Table S-4).

The six SOB genera detected catalyze different pathways; two genera contained genes for cSOx alone (*Thiovirga* and *Sulfurovum*), one S_4I alone (*Sediminibacterium,* as indicated by *tsdA*), and two had both cSOx and S_4I (*Halothiobacillus* and *Thiomonas*) pathways (Fig. 3b). Genes for the iSOx and rDSR pathways were only present in the genus *Thiobacillus,* where they were accompanied by the S_4I pathway, although genes for the rDSR pathway segment was also hosted by *Desulfurivibrio* (Fig. 3b). The NDFO genera, *Acidovorax*, possessed *ttrABC* which codes for tetrathionate reductase ($S_4O_6^{2-}$), an enzyme that reduces tetrathionate to thiosulfate, along with traces of the rDSR pathway system (Fig. 3b). The metagenomic inferences for these eight sulfur metabolizing genera were based on previous whole genome characterization of SOB from this tailings impoundment (Whaley-Martin et al. 2023).

During the experimental phase (28 days, Sep 22–Oct 19, 2020; Fig. 1b), sulfur metabolizing bacteria comprised 0.1–21.9% of the mesocosm communities, with a median sulfur metabolizing bacteria abundance of 1.6% (Fig. 3a). The varied tailings and thiosulfate pre-treatments resulted in divergent initial communities at day_0, with a higher mean total abundance of sulfur metabolizing bacteria occurring in mesocosms pre-treated with thiosulfate prior to the experimental phase (4.6% for E_1–E_5) than in those which received no pre-treatment (0.3% for E_6–E_8; Fig. 3a). At the beginning of the experimental stage (day_0), *Thiomonas* dominated six of the mesocosms (> 50% of the sulfur community in E_2, E_4–E_8, Fig. 3a, supplemental Table S-5). The sulfur metabolizing communities in the eight mesocosms diverged with time, with only mesocosm E_5 remaining dominated by *Thiomonas* on day_{28} (> 97% of sulfur bacteria), indicating that communities changed independently (Fig. 3a).

Mesocosms E_5 and E_6 (two of the thiosulfate-amended mesocosms) remained with *Thiomonas* (cSOx and S_4I) in the majority (> 50% of the SOB population) throughout the course of the experiment. However, the nitrate addition to

Table 2 Estimated proportion of time nitrate could be the terminal electron acceptor (TEA) based on the observed O_2 concentrations[a]

Mesocosm	Treatment	Sum of all periods DO below 0.5 mg/L (days)	Fraction of 28-day experiment with DO below 0.5 mg/L (%)
E_1	$T_{12}S_{4(2.0)}$	5.4	19
E_2	$T_{12}S_{4(2.0)}N_{2.0}$	4.2	15
E_3	$T_{12}S_{2(2.0)}$	16.5	59
E_4	$T_{12}S_{2(2.0)}N_{2.0}$	8.8	31
E_5	$S_{2(2.0)}$	6.9	25
E_6	$S_{2(2.0)}N_{2.0}$	0	0
E_7	T_{12}	3.5	13
E_8	$T_{12}N_{2.0}$	8.1	30

[a] $[NO_3^-] > 0.04$ mM throughout entire time course in all mesocosms

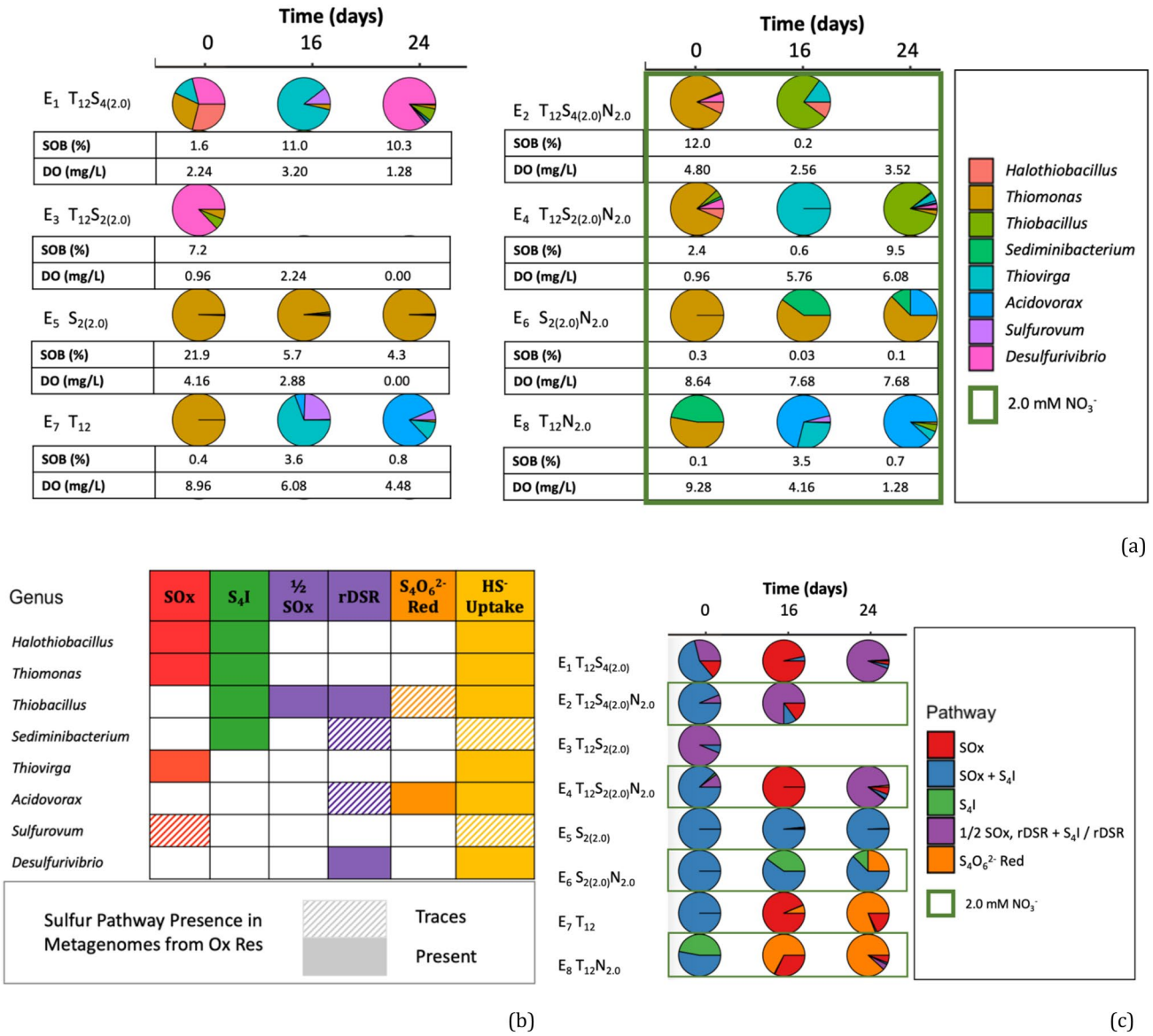

Fig. 3 **a** Relative abundance of the sulfur metabolizing bacteria across the 8 mesocosms for up to three timepoints. Reported oxygen concentrations observed at the lowest mesocosm water depth (90 cm depth) and fraction of the sulfur against total community are provided for each sampling timepoint available. **b** The sulfur pathways detected in sulfur metabolizing bacteria. Diagonal hatching (traces) indicates < 50% of the metagenomes sequenced contained one or more gene from the incomplete pathway, while solid colours indicate the complete sulfur pathway in most (> 70%) of all metagenomes sequenced; white squares indicate no genes associated with the pathway were detected (see SI Table 4) Note; the gene tsdA here was used to infer presence of the S_4I pathway. **c** The relative abundance of the sulfur genera which contain each pathway in their metagenomes. When more than one pathway is listed, sulfur metabolizing bacteria present within the community contain the capacity to activate either or both (i.e., cSOx + S_4I; iSOx, rDSR + S_4I or rDSR) pathways, and all have the capacity to uptake HS^-

the thiosulfate amendment (E_6) was linked to an increase in *Sediminibacterium* (S_4I) abundance from < 1% at day_0 to 42% by day_{16}, and *Acidovorax* (*ttrABC*) abundance from < 1% day_0 to 34% by day_{24} (Fig. 3). Mesocosms E_2 and E_4 (tailings, sulfur substrate (tetrathionate or thiosulfate), and nitrate (tetrathionate in E_2 and thiosulfate in E_4) transitioned from *Thiomonas*-dominated communities (cSOx and S_4I) to communities dominated by *Thiobacillus* (iSOx + rDSR, and S_4I).

Mesocosms E_1 and E_3 (tailings and sulfur substrate-amended without nitrate mesocosms) became dominated by *Desulfurivibrio* (rDSR) as the most abundant sulfur cycling genera. Although time series data are missing for E_3, the fraction of *Desulfurivibrio* in E_1 increased in relative

abundance for both the sulfur metabolizing and total microbial community (Fig. 3; Table S-5). Mesocosms E_7 and E_8 (tailings only) shifted from *Thiomonas* (cSOx and S_4I) dominance to a community where, by day_{16}, *Thiovirga* and *Sulfurovum* (cSOx) were dominant (E_7) or present (E_8). These communities then became dominated by *Acidovorax* (81% in E_7 and 88% in E_8) by day_{24}, indicating a potential shift from thiosulfate oxidation to tetrathionate reduction as thiosulfate concentrations were depleted (Fig. 3c).

Gene Expression: Sulfur Enzyme Trends (mRNA)

Pathway expression, as characterized by mRNA expression frequency, varied among the treatments (Fig. 4). Several trends emerged that were consistent with those identified in the 16S rRNA gene sequencing data (Fig. 3). The highest frequency of cSOx pathway expression along with low of S_4I pathway activity (*tsdA* expression frequency < 20) were detected in the mesocosm that received only an amendment of thiosulfate (E_5), consistent with the pathways inferred from 16S rRNA analysis (Fig. 4). In mesocosm E_6, S_4I pathway presence was indicated by the 16S rRNA analysis (*Thiomonas* and *Sediminibacterium*; Fig. 3), and the highest frequency of expression for the S_4I Pathway Part 1 (*tsdA*) was detected (Fig. 4). In mesocosm E_4, where *Thiobacillus* was found to dominate the 16S rRNA gene sequencing (Fig. 3), mRNA for the iSOx pathway was observed, although only traces of the rDSR pathway were expressed (Fig. 4). The mRNA signal for E_2 at day_{24} was faint but did not clearly indicate iSOx nor rDSR, instead suggesting the cSOx pathway.

In mesocosms E_1 and E_3, where *Desulfurivibrio* indicated presence of the rDSR pathway, mRNA expression also indicated that several rDSR genes were active, along with the tetrathionate reductase *ttrABC* ($S_4O_6^{2-}$ reduction), and the cSOx pathway (Fig. 4). Finally, mesocosms E_7 and E_8, which contained capacity for cSOx, S_4I and tetrathionate reduction (*ttrABC*), also displayed partial expression of these pathways—although *ttrABC* expression was only detected in E_8 (Fig. 4).

Gene Expression: Nitrogen Enzyme Trends (mRNA)

Expression of nitrogen processing genes lends some insight into the potential role of nitrate as a TEA (Fig. 4b). Genes for enzymes which reduce nitrate to nitrite (*narIGH* or *napAB* are required for dissimilatory nitrate reduction) were expressed in all mesocosms, with lowest expression in the thiosulfate, tailings and nitrate amended (E_4), and highest in the mesocosm treated with tailings and nitrate, but no sulfur amendment (E_8). The mRNA data does not clearly link nitrate reduction with sulfur pathway expression; since *nar* gene expression was high (> 100) at timepoints in E_1 and E_3 where rDSR pathway expression was detected, but also in E_5, where it was not (Fig. 4b). Expression of *nirB* in E_2-E_7 may suggest further conversion of nitrite to ammonia, while *nir* and *nor* expression in E_1, E_2, E_3 and E_8, may indicate that nitrous oxide was also produced; however, no information was available on the expression frequency of *nosZ*, which would further convert the nitrous oxide to $N_{2(g)}$ (Fig. 4b). Nitrogen fixation in the mesocosms was not supported, with only low and fragmented expression of the *nif* genes (Fig. 4b).

Discussion

Diagnostic Assessment Approach to Constrain the Active Sulphur Pathway(s)

To identify trends in sulfur pathway use, the three lines of evidence (geochemical, 16S rRNA linked to metagenomes, and mRNA results) were summarized in binary form (i.e. yes/no; Table 3). This new diagnostic approach draws from an extensive literature review summarized the reactions catalyzed by each of the three known sulfur pathways (Table S-1). Here, we identified six individual segments of those pathways (constrained genes with known geochemical outcomes) as key units of pathway occurrence (cSOx, iSOx, S_4I Part 1, S_4I Part 2, ttrABC, and rDSR). As the field of sulfur enzyme literature grows, this approach can be refined through the addition of other constrained sulfur enzyme systems.

By applying this approach to the mesocosm study, it was possible to discern trends in sulfur pathway activity. Results of the independent assessment for each mesocosm using the binary approach are shown in Table 3. The strength of the approach is apparent when considering the observed inconsistencies/ambiguities that arose when each line of evidence was considered separately. These may reflect the presence of "uncharacterised" sulfur metabolizing bacteria, (b) possible degradation of mRNA and 16S rRNA samples, and/or (c) loss or transformation of sulfur species prior to quantification. Here, alignment of these independent lines of evidence, clarifies which pathway(s) occur, even in the presence of data gaps.

The thiosulfate amended mesocosm, E_5, displayed all indicators (16S rRNA, mRNA, and geochemical) of the cSOx pathway (hosted by *Halothiobacillus*, *Thiomonas, Thiovirga* and *Sulfurovum*), and highest levels of cSOx mRNA expression. Here, thiosulfate amendments appear to promote dominance of the cSOx pathway, under conditions which are mostly, but not exclusively, oxic (Fig. S-1). However, since the proton yield in these mesocosms did not match that predicted by the complete cSOx pathway, and *tsdA* expression was detected, it seems that the S_4I Part 1

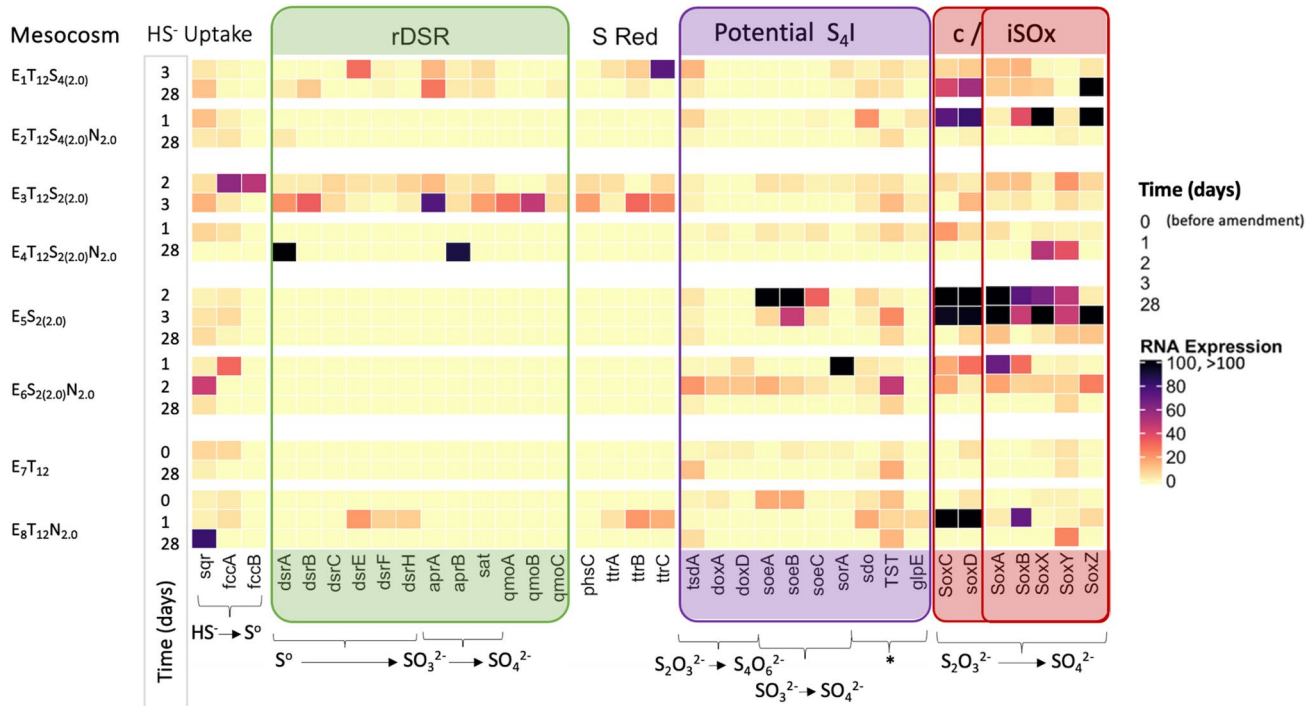

(a)

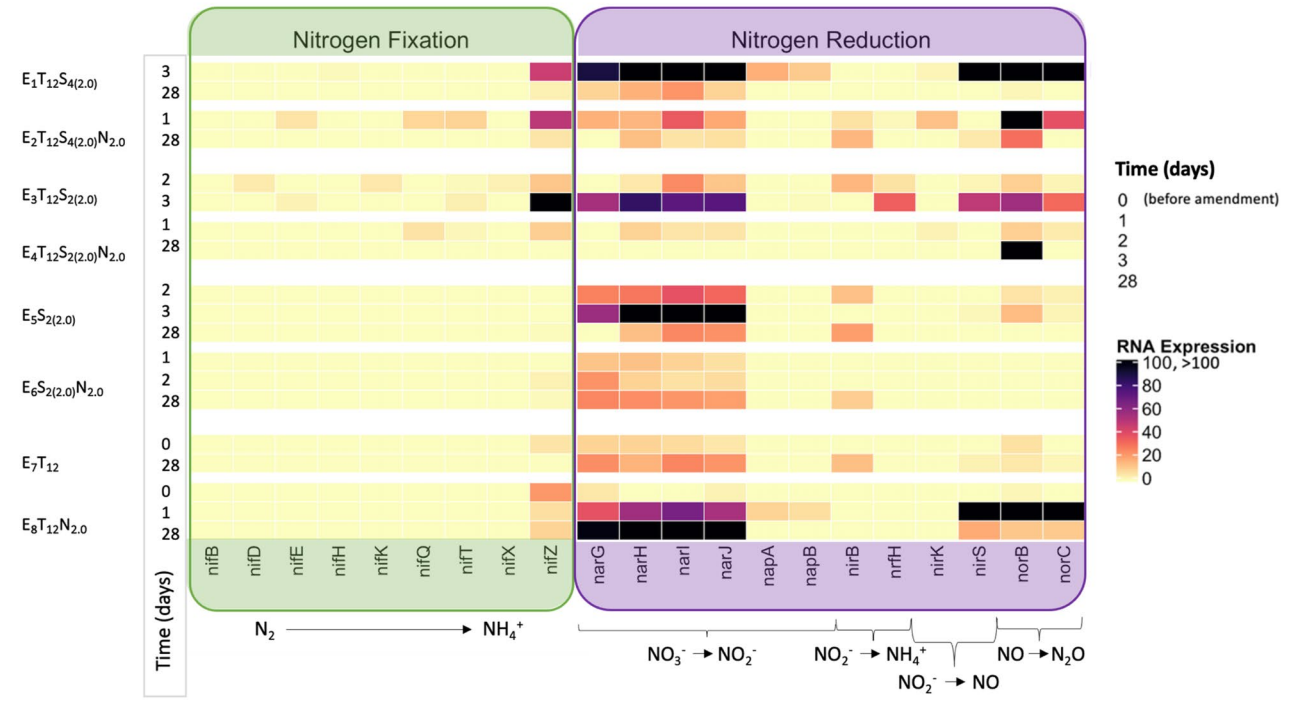

(b)

Fig. 4 A heat map of mRNA expression profile based on metatranscriptomic analysis. The values (in reads per kilobase million of transcript [RPKM] indicating transcriptomal activity, with darker squares indicate greater expression) were grouped by **a** sulfur cycling enzyme system (sulfide uptake, rDSR, sulfur reduction, potential S_4I, cSOx), and **b** nitrogen metabolism grouped by enzyme system. Additional variables including time (days) and treatments (colour legend on right) were paired to treatment parameters (without and with 2.0 mM nitrate (green bar) in addition to the sulfur and tailings amendments). (*) functions of Sdo, TST, and GplE remain to be clarified but may facilitate: Sdo ($S^0 \rightarrow SO_3^{2-}$), TST ($S_2O_3^{2-} \rightarrow SO_3^{2-}$), and GplE (sulfurtransferase, $S_2O_3^{2-} \rightarrow SO_3^{2-}$, SI Table 1). Gene expression data for *tetH* (S_4I Part 2) and *nosZ* were not available

Table 3 Lines of evidence supporting sulfur metabolizing pathways and nitrate as a TEA

Pathway / Indicators	Mesocosms							
	E_1	E_2	E_3	E_4	E_5	E_6	E_7	E_8
	$T_{12}S_{4(2.0)}$	$T_{12}S_{4(2.0)}N_{2.0}$	$T_{12}S_{2(2.0)}$	$T_{12}S_{2(2.0)}N_{2.0}$	$S_{2(2.0)}$	$S_{2(2.0)}N_{2.0}$	T_{12}	$T_{12}N_{2.0}$
Complete SOx ($S_2O_3^{2-} \rightarrow 2\ SO_4^{2-}$)								
pH decrease*	✓	✓	✓		✓			✓
cSOx pathway containing bacteria (*Thiomonas*, *Halothiobacillus*, *Thiovirga*, *Sulfurovum*) >10 % sulfur metabolizing community	✓	✓		✓	✓	✓	✓	✓
soxCD genes expressed in mRNA	✓	✓	✓		✓		✓	✓
Incomplete SOx ($S_2O_3^{2-} \rightarrow SO_4^{2-} + S^0$)								
pH stable*				✓			✓	
iSOx pathway containing bacteria (*Thiobacillus*) >10 % sulfur metabolizing community	<10 %	✓	<10 %	✓				
SOx genes expressed but *soxCD* absent (mRNA)				✓		✓	✓	
[S^0] increase *	✓	✓	✓	✓	✓	✓	✓	✓
S_4I Part 1 ($2\ S_2O_3^{2-} \rightarrow S_4O_6^{2-}$)								
pH increase or stable*				✓		✓	✓	
S_4I pathway containing bacteria *(Halothiobacillus*, *Thiomonas*, *Thiobacillus* and/or *Sediminibacterium*) >10 % sulfur metabolizing community	✓	✓		✓	✓	✓	✓	✓
tsdA or *doxDA* expressed in mRNA	✓	✓	✓	✓	✓	✓	✓	✓
[$S_4O_6^{2-}$] increase			✓	✓	✓	✓	✓	✓
S_4I Part 2 ($S_4O_6^{2-} \rightarrow 4\ SO_4^{2-}$)								
[$S_4O_6^{2-}$] decrease*	✓		✓					
tetH containing bacteria (*Thiobacillus*) >10 % sulfur metabolizing community		✓		✓				
ttrABC ($S_4O_6^{2-} \rightarrow 2\ S_2O_3^{2-}$)								
pH decrease*	✓	✓	✓		✓			✓
ttrABC containing bacteria (*Thiobacillus, Acidovorax*) >10 % sulfur metabolizing community	✓	✓	✓	✓		✓	✓	✓
ttrABC genes expressed in mRNA	✓		✓					✓
[$S_4O_6^{2-}$] decrease*	✓		✓					
rDSR ($S^0 \rightarrow SO_4^{2-}$)								
pH decrease*	✓	✓	✓		✓			✓
Thiobacillus, Desulfurvibrio abundance >10 % sulfur metabolizing community	✓	✓	✓	✓				
rDSR genes expressed in mRNA	✓	✓	✓	✓				✓
[S^0] decrease	✓	✓		✓				✓
Nitrate as a TEA								
Acidovorax or *Desulfurivibrio* (obligate anaerobes) >10 % sulfur metabolizing community	✓		✓			✓	✓	✓
Low oxygen concentrations (<0.5 mg/L) 10 – 60 % of time	✓	✓	✓	✓	✓		✓	✓
Nitrate present (i.e. > 0.04 mM)	✓	✓	✓	✓	✓	✓	✓	✓
Nitrate high (i.e. > 1.0 mM)		✓		✓		✓		✓
nar / nap genes expressed in mRNA	✓	✓	✓	✓	✓	✓	✓	✓

Table 3 (continued)

✓ Indicates Condition Met

✓ Indicates Traces of the Indicator Present

*Some signals such as pH changes or increases in SO_4^{2-} or S^0 concentrations are not uniquely associated with a single pathway. For example, S^0 may result from the iSOx pathway and/ or S_4I pathway P2

Note: all pathways require thiosulfate depletion – observed in all mesocosms, see reaction rates (SI Table 5)

Table 4 Theoretical vs. actual proton yield from amendment ($day_{1.25}$) to end (day_{28})

Mesocosm	$\Delta S\text{-}S_2O_3^{2-}$ (µM)	Predicted ΔH^+ (µM) if cSOx[a]	Actual ΔH^+ (µM)
E_1	− 550	550	5.6
E_2	− 320	320	1.1
E_3	− 1750	1750	0.8
E_4	− 1060	1060	− 5.7
E_5	− 1670	1670	1.3
E_6	− 940	940	− 7.9
E_7	− 340	340	0.0
E_8	− 490	490	0.8

[a]When the calculations of protons released were reduced by the number of moles of S which were converted into either tetrathionate (S_4I pathway) or elemental sulfur (iSOx or S_4I pathway), and the proton sink of thiosulfate to tetrathionate conversions were accounted for, the predicted ΔH^+ remained in the same order of magnitude as cSOx predictions (above), so were insufficient to explain the actual ΔH^+

pathway—while not dominant—was active as a secondary metabolism (hosted by *Halothiobacillus*, *Thiomonas*, *Thiobacillus, Thiovirga*, *Acidovorax,* and/or *Sediminibacterium*).

Second, in E_6, both the highest frequency of *tsdA* expression and largest -ΔH^+ were detected, consistent with S_4I Part 1 pathway dominance (Tables 3, 4). E_6 also saw an increase in the genus *Sediminibacterium*, which hosts the S_4I, but not the cSOx, pathway. Here, S_4I pathway dominance appears to be a response to the availability of thiosulfate, oxygen, and possibly nitrate (E_6 began with 1.39 mM $S_2O_3^{2-}$, and 1.77 mM NO_3^{2-}, Table 3); since overall SOB populations constituted a lower fraction of the overall population with nitrate amendments (Fig. 1), it is possible that the nitrate amendments stimulated competition from N-metabolising parts of the community, causing competition for resources with bacteria hosting the cSOx pathway.

In addition to E_5, three other mesocosms displayed all indicators for cSOx pathway activity (E_1, E_2 and E_8), while E_3 displayed some indicators of the cSOx pathway, except for the detection of an abundant host genus (see Table 4). Two other mesocosms also contained all indicators for activity of the first stage of the S_4I pathway (E_4 and E_7; Table 4). Notebly, unambiguous indicators of the S_4I pathway Part 2 remain to be identified (Tanabe and Dahl 2022; Zhang et al. 2020).

In addition to indicators for activity of other pathways, mesocosm E_4, alone (exposed to tailings, thiosulfate, and nitrate), displayed all indicators of the iSOx pathway, found in *Thiobacillus*, along with traces of the rDSR pathway in the mRNA. The remaining mesocosms (E_1 and E_3: tailings, tetrathionate, thiosulfate, and ambient nitrate) contained the indicators for the tetrathionate reductase *ttrABC*, and most (E_3) or all (E_1) for the rDSR pathway (Table 4).

Finally, mesocosms E_7 and E_8, which contained microbes with capacity for cSOx, S_4I were found to indicate cSOx for E_8, and S_4I for E_7 as described above. The potential for the community in E_8 to facilitate tetrathionate reduction (*ttrABC* presence and expression) was not matched by a geochemical signal (tetrathionate loss), and so remains ambiguous.

Sulfur-Driven Acidity: Theoretical vs. Observed

To examine the effectiveness of the diagnostic strategy proposed above to identify possible sulfur pathways operating (Table 3), acidity generation relative to *soxCD* expression (required for the cSOx pathway, producing H^+ and sulfate) was evaluated (Fig. 5). Consistent with immediate acid generation associated with the cSOx pathway, a positive relationship between *soxCD* activity (mRNA expression frequency) and proton yield (ΔH^+) occurred in five of the eight mesocosms. Mesocosms E_4, E_6 and E_7, by contrast, developed a negative proton yield ($-\Delta H^+$) consistent with activation of the first portion of the S_4I pathway (*tsdA*; see Table S-1). In particular, E_6 displayed the largest $-\Delta H^+$ and the highest frequency of *tsdA* expression. Here, we assumed expression frequencies of <25 were not significantly different from zero (i.e. background signal noise or contamination). Further work may better define a robust cut-off point to discriminate minimum *soxCD* expression and other pathway genes.

Since *soxCD* genes were active in five of the eight mesocosms, we compared the theoretical proton yields that would arise from thiosulfate oxidation by the cSOx pathway (i.e. 1 mol of H^+ generated from 1 mol of per mole of $S\text{-}S_2O_3^{2-}$, (Eq. 1; Friedrich et al. 2001) with the actual proton yields calculated from the change in pH from $day_{1.25}$ to day_{28} (Table 4). Actual proton yields were found to be much lower than theoretical across all mesocosms (Table 4). The relationship between ΔH^+ and ΔSO_4^{2-} across all treatments was also extremely poor (Pearson $r = 0.066$, $P = 0.88$; see supplemental Fig. S-2). Indeed, the observed acid generation could

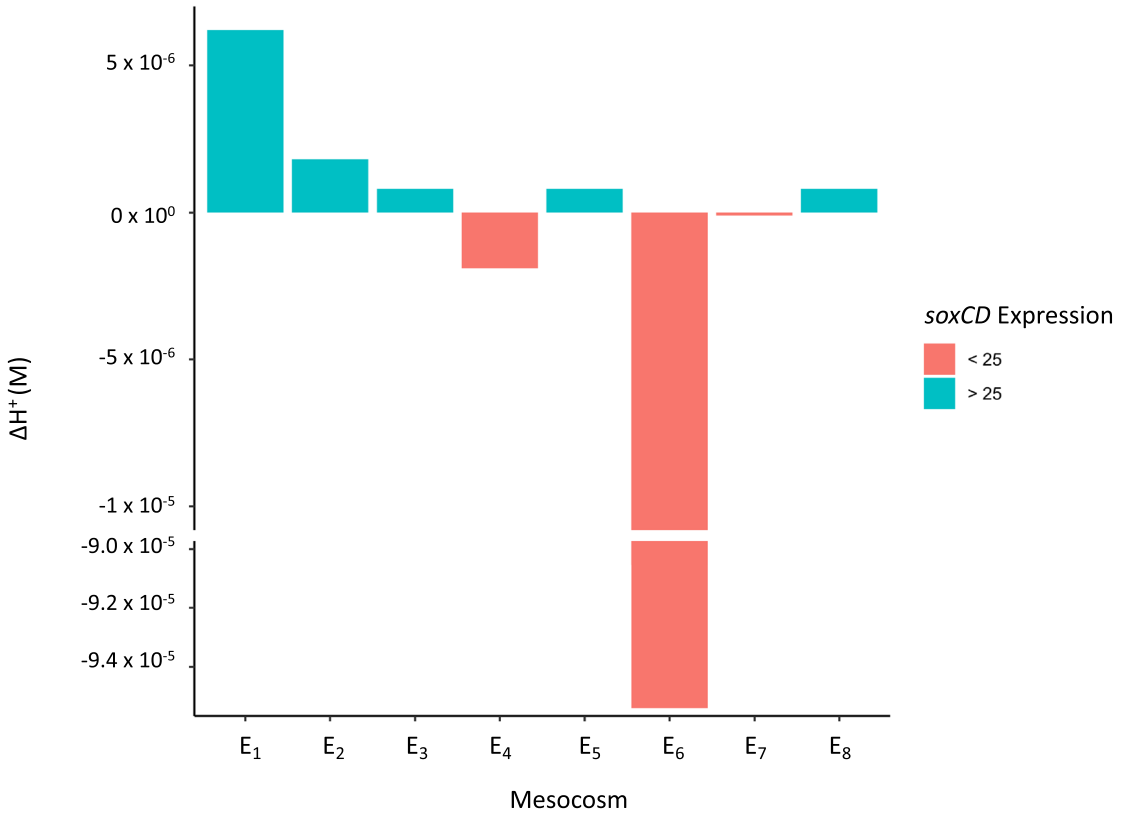

Fig. 5 The net proton yield for the 8 mesocosms over the course of the experiment versus the gene expression of *soxCD* (>25 mean mRNA frequency detected at least once during the experiment), indicating the use of the complete vs. incomplete SOx pathway. Note the y-axis break between -1.0×10^{-5} and -9.0×10^{-5} M

be accounted for by oxidation of only 0.1–1% of the thiosulfate to sulfate via the cSOx pathway, a scenario deemed unlikely (supplemental Table S-6), and alkalinity did not account for the discrepancies (see above).

To account for the proton yield discrepancies, it was reasoned that there must be one, or more, proton sink reaction(s) that co-occurred alongside the acid generated via the cSOx pathway. While acidity generation was clearly linked to sulfur oxidation in the mesocosms, it is also possible that other independent cellular processes acted as proton sinks. These processes, for example, could include cell synthesis (Eq. 5), nitrogen fixation (Eq. 6), or nitrate reduction (Eq. 7) (Rittmann and McCarty 2001):

$$1/2CO_2 + 1/20\ NH_4^+ + 1/20\ HCO_3^- + H^+ + e^- \rightarrow 1/20\ C_5H_7O_2N + 9/20\ H_2O \quad (5)$$

$$N_2 + 8H^+ + 8e^- + 16ATP \rightarrow 2NH_3 + H_2 + 16ADP + 16P_i \quad (6)$$

$$5C_6H_{12}O_6 + 24NO_3^- + 24H^+ \rightarrow 30CO_2 + 42H_2O + 12N_2 \quad (7)$$

However, if we assume that proton consuming reactions, like the proton generating ones, were linked to sulfur metabolism, the low rates of acid production suggest that proton consuming and producing sulfur oxidizing reaction(s) approximately neutralized each other. Proton consuming sulfur reactions are known to be used by SOB, such as the S_4I Part 1 pathway (*tsdA*) paired with oxygen (facilitated, for example, by *Thiomonas* or *Halothiobacillus*), or the iSOx pathway (lacking SoxCD) paired with nitrate (facilitated by *Thiobacillus*, see Table S-1).

Simultaneous Thiosulfate Oxidation through Multiple Pathways

Simultaneous activity of proton-generating and -consuming reactions would have the benefit of minimizing pH changes in the cytoplasm, reducing the energetic cost to maintain homeostasis. Potential matching of proton generating and consuming processes, could include cSOx + S_4I Part 1, or S_4I Part 1 + S_4I Part 2 (Table S-1). To explore if simultaneous pathway activation could account for observed proton yields, eight acid generation scenarios were simulated

(Table S-6). Each scenario consisted of a different proportions of thiosulfate oxidation through cSOx, S_4I and iSOx pathways (for simplicity, consistent fractions were assumed over the 28 days of the experiment, see Table S-6). Theoretical sulfur oxidation scenarios best fitting actual detected ΔH^+ included combinations such as 34% cSOx + 66% S_4I (matching potential pathways detected in E_5 and E_6, see Fig. 3) or 17% cSOx + 33% S_4I + 50% iSOx (pathways detected in mesocosms E_1–E_4, see Fig. 4), further suggesting simultaneous activity of the cSOx and S_4I pathways.

Indeed, concurrent use of the cSOx and S_4I pathways has been previously observed in several studies. *Paracoccus thiocyanatus SST* was observed to activate both pathways simultaneously (Rameez et al. 2020), although in that study, pH changes were not balanced between the two (10% cSOx, 90% S_4I Part 1 led to net pH increase). Similarly, enzymes suggesting the parallel activation of the cSOx and potential later steps of the S_4I pathway (*sorAB*) were also observed in the SOB bacterium *Starkeya novella* (formerly known as *Thiobacillus novellus*) when fed 40 mM thiosulfate (Kappler et al. 2001). Further, thiosulfate oxidation by the iSOx (lacking SoxCD) plus rDSR, at the same time as the S_4I pathway, was found to be possible in *Allochromatium vinosum*, where thiosulfate led to concurrent generation of sulfate (formed by upregulation of both iSOx and rDSR pathways) and tetrathionate (via the S_4I pathway Part 1; Hensen et al. 2006). Together, these studies suggest that simultaneous pathway activation is possible, or even common, in SOB. However, little research exists to suggest when these pathways are activated together, and if their parallel use by specific SOB is employed as a strategy to minimize pH changes in their cytoplasm or aquatic environment.

However, when the proton consuming side reactions accounting for the [S^0] and [$S_4O_6^{2-}$] detected in the mesocosms were added to the theoretical acid yields model, they did not appreciably reduce predicted proton yields (Table 4). It is possible that this is due to an underestimation of proton uptake by *tsdA*, because actual [$S_4O_6^{2-}$] were greater than those measured owing to losses during prolonged sample storage (> 1 year), and/or an underestimation of S^0 formation if excreted extracellular sulfur globules settled to the bottom of the mesocosms. Alternately, the proportion of the S_4I pathway may also have been underestimated if $S_4O_6^{2-}$, once formed, continued to be oxidized via an acid neutral or proton consuming second stage of the S_4I pathway (generating undetected SOIs), or reduced to thiosulfate via *ttrABC*. Unaccounted for S contributed from ≈ 0–43.2% of the sulfur mass balance, indicating additional unidentified SOI compounds were present.

The enzymes facilitating the latter half of the S_4I pathway remain unclear (Rameez et al. 2020), and may occur in one or more stages (Eq. 8):

$$S_4O_6^{2-} + 3.5O_2 + 3H_2O \rightarrow 4SO_4^{2-} + 6H^+ \quad (8)$$

Some research suggests that $S_4O_6^{2-}$ disproportionation occurs as part of the S_4I pathway, leading to ZVS formation (supplemental Table S-1). The mechanism is sometimes attributed to *tetH* or *TTH*, a gene detected in the metagenomes of *Thiobacillus* spp. found in the tailings impoundment used as source water for this study (Beard et al. 2011; Camacho et al. 2020a). Alternately, research on the SOB *Erythrobacter flavus*, suggest that in this species the genes *tsdA* and *soxB* play a role in S^0 formation via the S_4I pathway (Zhang et al. 2020). Future research is required to determine whether tetrathionate oxidation occurs in a single enzyme facilitated step, or over two or more; a multi-step process would allow formation of other sulphur intermediates (pH neutral) before the onset of rapid acid generation, a phenomenon observed in preliminary mesocosm studies onsite in 2019 (unpublished data).

Nitrate as a Possible Alternative to Oxygen for Sulfur Oxidation

Over the course of this experiment, oxygen fell below a conservative estimate of the concentration above which oxygen is exclusively used (0.5 mg/L, or 0.0156 mM) for approximately 1/3 of the duration, in all mesocosms except E_6. Nitrate, always present in all mesocosms at > 0.04 mM, is also abundant in the tailings impoundment onsite (0.017–0.156 mM; Whaley-Martin et al. 2023).

When nitrate is the terminal electron acceptor, the theoretical H^+ yield is considerably lower. This has an impact on the $\Delta H^+/\Delta S$–$S_2O_3^{2-}$ ratio for any of the cSOx, complete S_4I, or iSOx and rDSR pathways (see Table S-1). For example, with oxygen, the net proton yield of each is 1 mol of H^+ generated from 1 mol of S–$S_2O_3^{2-}$ oxidation (Eq. 9), while with nitrate, the net drops to 0 mol H^+ generated from 1 mol S–$S_2O_3^{2-}$ oxidation (Eq. 10):

$$S_2O_3^{2-} + 1H_2O + 2O_2 \rightarrow 2SO_4^{2-} + 2H^+ \quad \Delta H^+/\Delta S = 1 \quad (9)$$

$$S_2O_3^{2-} + 2H_2O + NO_3^- \rightarrow 2SO_4^{2-} + NH_4^+ \quad \Delta H^+/\Delta S = 0 \quad (10)$$

As a result, low oxygen conditions which favour nitrate pairing reduce the proton yield as reactive sulfur compounds are oxidized. Periods of low oxygen concentrations were detected in seven of the eight mesocosms, and E_8 displayed all indicators of NO_3^- reduction (Table 3). Yet, here, observed NO_3^- loss was not equalled by increases in NH_4^+, adding ambiguity that might be explained by heterotrophic activity (e.g. ammonia uptake) and possibly autotrophic nitrogen fixation (although this was not supported by mRNA, as the *nif* genes were not active).

Signals of nitrate use from the sulfur metabolizing community (16S rRNA and mRNA) are more suggestive.

Reports in the literature list *Halothiobacillus* (cSOx and S_4I), *Thiovirga* (cSOx), *Thiomonas* (cSOx and S_4I), and *Sediminibacterium* as strictly aerobic (Arsène-Ploetze et al. 2010; Chen et al. 2004; Kang et al. 2014; Kim et al. 2016; Sievert et al. 2000; Song et al. 2017; Wood et al. 2005); *Acidovorax* ($S_4O_6^{2-}$ Red) and *Desulfurivibrio* (rDSR) as strictly anaerobic (Pantke et al. 2012; Carlson et al. 2013; Thorup et al. 2017; Sun et al. 2022); and *Thiobacillus* (iSOx, rDSR, and S_4I) and *Sulfurovum* (cSOx) as facultative anaerobes (Beller et al. 2006; Ghosh and Dam 2009; Inagaki et al. 2004; Jong et al. 1997; Meier et al. 2017; Mori et al. 2018 [supplemental Table S-7]). These categorizations are suggestive of nitrate use, although exceptions exist. Whaley-Martin et al. (2023) classified *Halothiobacillus*, collected from the same tailings impoundment as this study as a strict aerobe, although some species contained partial *nir* and *nor* genes associated with nitrite reduction, a function also recently reported (Magnuson et al. 2023). Likewise, one species of *Thiomonas* has been reported to host a nitrate reductase gene, suggesting facultative anaerobic respiration may be available to some species in the genus (Arsène-Ploetze et al. 2010).

Strictly anaerobic *Acidovorax* ($S_4O_6^{2-}$ reduction) and *Desulfurivibrio* (rDSR) were detected in several mesocosms. As well, gene expression indicating nitrate use (*nap* and *nar* genes) was detected in all mesocosms; Mesocosm E_8 had particularly high gene expression towards the end of the experiment. In addition, the abundance of the facultative anaerobe *Thiobacillus* (containing the iSOx + rDSR pathway) appears to be linked to low oxygen availability and may indicate a pairing of nitrate with the rDSR pathway, as recently proposed (Whaley-Martin et al. 2023). Thermodynamic theory supports the pairing of nitrate with the iSOx + rDSR pathway (Klatt and Polerecky 2015). Other studies have discussed the presence of nitrate-dependant thiosulfate oxidation in *Thiobacillus denitrificans*; the studies note that it causes stored elemental sulfur globules, as ZVS formation is generally much more rapid than its subsequent oxidation (Jiang et al. 2009; Schedel and Trüper 1980; Zhang et al. 2019). In addition, *nap* and *nar* genes were found to be expressed in the microbial communities found in all mesocosms, which further indicates nitrate reduction. Whether used by strict or facultative anaerobes, nitrate pairing has the potential to reduce acidity if anoxic conditions are maintained; however, if the ZVS discharged is produced under anoxic conditions, exposure of ZVS-containing SOB to oxic conditions could result in acidity generation.

Conclusions

This study demonstrates how a new diagnostic approach integrating three lines of evidence collected at different frequencies (physiochemistry/geochemistry, 16S rRNA gene sequencing linked to metagenomes, and gene expression) enabled the identification of which microbial sulfur oxidation pathways were operating under varying environmental conditions and their influences on S geochemical outcomes. All three known sulfur biochemical pathways: complete sulfur oxidation (cSOx), tetrathionate intermediate (S_4I), and incomplete SOx (iSOx, lacking SoxCD) followed by reverse dissimilatory sulfate reduction (rDSR) were demonstrated to occur in the study of eight experimental mine wastewater mesocosms. This integrated assessment approach identified parallel pathway operation, which resulted in lower sulfate-acid ratios than those theoretically predicted. The approach thus offers a more complete story of tailings impoundment S geochemistry and the potential risks that it causes, as well as the factors associated with pathway dominance. Here, variations in conditions within concentration ranges commonly observed in active base metal mine tailings impoundment, led to cSOx pathway expression and parallel use of S_4I and/or iSOx pathways. Results linking the mRNA and ΔH^+ from these experiments also indicate that SoxCD is a potential indicator for direct oxidation and acid generation via the cSOx pathway, although the proton balance is moderated by other factors, such as multiple pathways activity and the use of nitrate by some sulfur oxidizing bacteria under low oxygen conditions.

Supplementary Information The online version contains supplementary material available at https://doi.org/10.1007/s10230-024-01016-x.

Acknowledgements The authors thank all of the on-site mine personnel who aided in site orientation, sample collection, and processing. Research was supported by the Genome Canada Large Scale Applied Research Program and Ontario Research Fund–Research Excellence grants to L.A.W. and J.F.B.

Data availability The metagenome-assembled genomes (MAGs) data referenced in this study are available at ggkbase.berkeley.edu via https://ggkbase.berkeley.edu/mine_tailing_impoundment_time_series.

References

Arsène-Ploetze F, Koechler S, Marchal M, Coppée J, Chandler M, Bonnefoy V (2010) Structure, function, and evolution of the *Thiomonas* spp. genome. PLoS Genet 6:e1000859. https://doi.org/10.1371/journal.pgen.1000859

Beard S, Paradela A, Albar JP, Jerez CA (2011) Growth of *Acidithiobacillus ferrooxidans* ATCC 23270 in thiosulfate under oxygen-limiting conditions generates extracellular sulfur globules by means of a secreted tetrathionate hydrolase. Front Microbiol. https://doi.org/10.3389/fmicb.2011.00079

Bell E, Lamminmäki T, Alneberg J, Andersson A, Qian C, Xiong W, Hettich R, Frutschi M, Bernier-Latmani R (2020) Active sulfur cycling in the terrestrial deep subsurface. ISME J. https://doi.org/10.1038/s41396-020-0602-x

Beller HR, Chain PSG, Letain TE, Chakicherla A, Richardson PM, Coleman MA, Wood AP, Kelly DP (2006) The genome sequence of the obligately chemolithoautotrophic, facultatively anaerobic bacterium *Thiobacillus denitrificans*. J Bacteriol 188:1473–1488. https://doi.org/10.1128/JB.188.4.1473-1488.2006

Camacho D, Frazao R, Fouillen A, Nanci A, Lang BF, Apte S, Baron C, Warren L (2020a) New insights into *Acidithiobacillus thiooxidans* sulfur metabolism through coupled gene expression, solution chemistry, microscopy, and spectroscopy analyses. Front Microbiol. https://doi.org/10.3389/fmicb.2020.00411

Camacho D, Jessen GL, Mori JF, Apte SC, Jarolimek CV, Warren LA (2020b) Microbial succession signals the initiation of acidification in mining wastewaters. Mine Water Environ 39:669–683. https://doi.org/10.1007/s10230-020-00711-9

Carlson HK, Clark IC, Blazewicz SJ, Iavarone AT, Coates JD (2013) Fe(II) oxidation is an innate capability of nitrate-reducing bacteria that involves abiotic and biotic reactions. J Bacteriol 195:3260–3268. https://doi.org/10.1128/JB.00058-13

Chen X-G, Geng A-L, Yan R, Gould WD, Ng YL, Liang DT (2004) Isolation and characterization of sulphur-oxidizing *Thiomonas sp.* and its potential application in biological deodorization. Lett Appl Microbiol 39:495–503. https://doi.org/10.1111/j.1472-765X.2004.01615.x

Cron BR, Sheik CS, Kafantaris FCA, Druschel GK, Seewald JS, German CR, Dick GJ, Breier J, Toner BM (2020) Dynamic biogeochemistry of the particulate sulfur pool in a buoyant deep-sea hydrothermal plume. ACS Earth Sp Chem 4:168–182. https://doi.org/10.1021/acsearthspacechem.9b00214

Dahl C (2005) A biochemical view on the biological sulfur cycle. In: Lens PNL (ed) Environmental Technologies to treat sulfur pollution—principles and applications, 2nd edn. IWA Publishing, London, pp 55–96

Dam B, Mandal S, Ghosh W, Das Gupta SK, Roy P (2007) The S4-intermediate pathway for the oxidation of thiosulfate by the chemolithoautotroph *Tetrathiobacter kashmirensis* and inhibition of tetrathionate oxidation by sulfite. Res Microbiol 158:330–338. https://doi.org/10.1016/j.resmic.2006.12.013

Duffy D, Garg S, Washer W, Grammatikopoulos T, Papangelakis V (2015) Mineralogical characterization of Sudbury pyrrhotite tailings: evaluating the bioleaching potential. Canadian Institute of Mining, Metallurgy and Petroleum conference paper. https://onetunnel.org/documents/mineralogical-characterization-of-sudbury-pyrrhotite-tailings-evaluating-the-bioleaching-potential

Friedrich CG, Bardischewsky F, Rother D, Quentmeier A, Fischer J (2005) Prokaryotic sulfur oxidation. Curr Opin Microbiol 8(3):253–259. https://doi.org/10.1016/j.mib.2005.04.005

Friedrich CG, Rother D, Bardischewsky F, Quentmeier A, Fischer J (2001) Oxidation of reduced inorganic sulfur compounds by bacteria: emergence of a common mechanism? Appl Environ Microbiol 67:2873–2882. https://doi.org/10.1128/AEM.67.7.2873-2882.2001

Ghosh W, Dam B (2009) Biochemistry and molecular biology of lithotrophic sulfur oxidation by taxonomically and ecologically diverse bacteria and archaea. FEMS Microbiol Rev 33:999–1043. https://doi.org/10.1111/j.1574-6976.2009.00187.x

Grettenberger CL, Havig JR, Hamilton TL (2020) Metabolic diversity and co-occurrence of multiple *Ferrovum* species at an acid mine drainage site. BMC Microbiol. https://doi.org/10.1101/751859

Gu Z, Eils R, Schlesner M (2016) Complex heatmaps reveal patterns and correlations in multidimensional genomic data. Bioinformatics 32:2847–2849. https://doi.org/10.1093/bioinformatics/btw313

Hensen D, Sperling D, Trüper HG, Brune DC, Dahl C (2006) Thiosulphate oxidation in the phototrophic sulphur bacterium *Allochromatium vinosum*. Mol Microbiol 62:794–810. https://doi.org/10.1111/j.1365-2958.2006.05408.x

Inagaki F, Takai K, Nealson KH, Horikoshi K (2004) *Sulfurovum lithotrophicum* gen. nov., sp. nov., a novel sulfur-oxidizing chemolithoautotroph within the ε-Proteobacteria isolated from Okinawa Trough hydrothermal sediments. Int J Syst Evol Microbiol 54:1477–1482. https://doi.org/10.1099/ijs.0.03042-0

Jiang G, Sharma KR, Guisasola A, Keller J, Yuan Z (2009) Sulfur transformation in rising main sewers receiving nitrate dosage. Water Res 43:4430–4440. https://doi.org/10.1016/j.watres.2009.07.001

Jin Q, Kirk MF (2018) pH as a primary control in environmental microbiology: 1. Thermodynamic perspective. Front Environ Sci 6:1–15. https://doi.org/10.3389/fenvs.2018.00021

Jong GAH, Hazeu W, Bos P, Kuenen JG (1997) Isolation of the tetrathionate hydrolase from *Thiobacillus acidophilus*. Eur J Biochem 243:678–683. https://doi.org/10.1111/j.1432-1033.1997.00678.x

Kang H, Kim H, Il LB, Joung Y, Joh K (2014) *Sediminibacterium goheungense* sp. nov., isolated from a freshwater reservoir. Int J Syst Evol Microbiol 64:1328–1333. https://doi.org/10.1099/ijs.0.055137-0

Kappler U, Friedrich CG, Trüper HG, Dahl C (2001) Evidence for two pathways of thiosulfate oxidation in *Starkeya novella* (formerly *Thiobacillus novellus*). Arch Microbiol 175:102–111. https://doi.org/10.1007/s002030000241

Kim Y, Kim B, Kang K, Ahn TY (2016) *Sediminibacterium aquarii* sp. nov., isolated from sediment in a fishbowl. Int J Syst Evol Microbiol 66:4501–4505. https://doi.org/10.1099/ijsem.0.001380

Klatt JM, Polerecky L (2015) Assessment of the stoichiometry and efficiency of CO_2 fixation coupled to reduced sulfur oxidation. Front Microbiol 6:484. https://doi.org/10.3389/fmicb.2015.00484

Lipps WC, Braun-Howland EB, Baxter TE (2023) Standard Methods for the Examination of Water and Wastewater. 24th Edition, American Public Health Assoc, American Water Works Assoc, Water Environment Federation, APHA Press, Washington D.C

Magnuson E, Altshuler I, Freyria NJ, Leveille RJ, Whyte LG (2023) Sulfur-cycling chemolithoautotrophic microbial community dominates a cold, anoxic, hypersaline Arctic spring. Microbiome. https://doi.org/10.1186/s40168-023-01628-5

Martin M (2011) Cutadapt removes adapter sequences from high-throughput sequencing reads. Embnet J 17:10–12

Meier DV, Pjevac P, Bach W, Hourdez S, Girguis PR, Vidoudez C, Amann R, Meyerdierks A (2017) Niche partitioning of diverse sulfur-oxidizing bacteria at hydrothermal vents. ISME J 11:1545–1558. https://doi.org/10.1038/ismej.2017.37

Melton ED, Sorokin DY, Overmars L, Chertkov O, Clum A, Pillay M, Ivanova N, Shapiro N, Kyrpides N, Woyke T, Lapidus A, Muyzer G (2016) Complete genome sequence of *Desulfurivibrio alkaliphilus* strain AHT2T, a haloalkaliphilic sulfidogen from Egyptian hypersaline alkaline lakes. Stand Genomic Sci 11:67. https://doi.org/10.1186/s40793-016-0184-4

Miettinen H, Bomberg M, Le TMK, Kinnunen P (2021) Identification and metabolism of naturally prevailing microorganisms in zinc and copper mineral processing. Minerals 11:1–31. https://doi.org/10.3390/min11020156

Mori K, Yamaguchi K, Hanada S (2018) *Sulfurovum denitrificans* sp. nov., an obligately chemolithoautotrophic sulfur-oxidizing epsilonproteobacterium isolated from a hydrothermal field. Int J Syst Evol Microbiol 68:2183–2187. https://doi.org/10.1099/ijsem.0.002803

Nancucheo I, Bitencourt JAP, Sahoo PK, Alves JO, Siqueira JO, Oliveira G (2017) Recent developments for remediating acidic mine waters using sulfidogenic bacteria. Biomed Res Int 2017:7256582. https://doi.org/10.1155/2017/7256582

Nhantumbo C, Larsson R, Larson M, Juizo D, Persson KK (2018) A simplified model to simulate pH and alkalinity in the mixing zone downstream of an acidic discharge. Mine Water Environ 37:552–564. https://doi.org/10.1007/s10230-018-0515-3

Pantke C, Obst M, Benzerara K, Morin G, Ona-Nguema G, Dippon U, Kappler A (2012) Green rust formation during Fe(II) oxidation by the nitrate-reducing *Acidovorax sp*. Strain BoFeN1. Environ Sci Technol 46:1439–1446. https://doi.org/10.1021/es2016457

Rameez MJ, Pyne P, Mandal S, Chatterjee S, Alam M, Bhattacharya S, Mondal N, Sarkar J, Ghosh W (2020) Two pathways for thiosulfate oxidation in the alphaproteobacterial chemolithotroph *Paracoccus thiocyanatus* SST. Microbiol Res. https://doi.org/10.1016/j.micres.2019.126345

Rethmeier J, Rabenstein A, Langer M, Fischer U (1997) Detection of traces of oxidized and reduced sulfur compounds in small samples by combination of different high-performance liquid chromatography methods. J Chromatogr A 760:295–302. https://doi.org/10.1016/S0021-9673(96)00809-6

Rittmann BE, McCarty PL (2001) Environmental biotechnology: principles and applications. Curr Opin Biotechnol. https://doi.org/10.1016/S0958-1669(96)80047-4

Schedel M, Trüper HG (1980) Anaerobic oxidation of thiosulfate and elemental sulfur in *Thiobacillus denitrificans*. Arch Microbiol 124–124:205–210. https://doi.org/10.1007/BF00427728

Sievert SM, Heidorn T, Kuever J (2000) *Halothiobacillus kellyi* sp. nov., a mesophilic, obligately chemolithoautotrophic, sulfur-oxidizing bacterium isolated from a shallow- water hydrothermal vent in the Aegean Sea, and emended description of the genus *Halothiobacillus*. Int J Syst Evol Microbiol 50:1229–1237. https://doi.org/10.1099/00207713-50-3-1229

Skousen J, Zipper CE, Rose A, Ziemkiewicz PF, Nairn R, McDonald LM, Kleinmann RL (2017) Review of passive systems for acid mine drainage treatment. Mine Water Environ 36:133–153. https://doi.org/10.1007/s10230-016-0417-1

Song Y, Jia J, Liu D, Choi L, Wang G, Li M (2017) *Sediminibacterium roseum* sp. Nov., isolated from sewage sediment. Int J Syst Evol Microbiol 67:4674–4679. https://doi.org/10.1099/ijsem.0.002355

Sun X, Kong T, Li F, Häggblom MM, Kolton M, Lan L, Lau V, Maggie CY, Dong Y, Gao P, Kostka JE, Baoqin Li, Weimin S (2022) *Desulfurivibrio spp.* mediate sulfur-oxidation coupled to Sb(V) reduction, a novel biogeochemical process. ISME J 16:1547–1556. https://doi.org/10.1038/s41396-022-01201-2

Tanabe TS, Dahl C (2022) HMS-S-S: a tool for the identification of sulphur metabolism-related genes and analysis of operon structures in genome and metagenome assemblies. Mol Ecol Resour 22:2758–2774. https://doi.org/10.1111/1755-0998.13642

Thorup C, Schramm A, Findlay AJ, Finster KW, Schreiber L (2017) Disguised as a sulfate reducer: growth of the deltaproteobacterium *Desulfurivibrio alkaliphilus* by sulfide oxidation with nitrate. Mbio 8:1–9. https://doi.org/10.1128/mBio.00671-17

van Vliet DM, von Meijenfeldt FAB, Dutilh BE, Villanueva L, Sinninghe Damsté JS, Stams AJM, Sánchez-Andrea I (2021) The bacterial sulfur cycle in expanding dysoxic and euxinic marine waters. Environ Microbiol 23:2834–2857. https://doi.org/10.1111/1462-2920.15265

Verburg R, Bezuidenhout N, Chatwin T, Ferguson K (2009) The global acid rock drainage guide (GARD guide). Mine Water Environ 28:305. https://doi.org/10.1007/s10230-009-0078-4

Wang R, Lin JQ, Liu XM, Pang X, Zhang CJ, Yang CL, Gao XY, Lin CM, Li YQ, Li Y, Lin JQ, Chen LX (2019) Sulfur oxidation in the acidophilic autotrophic *Acidithiobacillus spp*. Front Microbiol 10:1–20. https://doi.org/10.3389/fmicb.2018.03290

Wang X, Zhang Y, Zhang T, Zhou J (2016) Effect of dissolved oxygen on elemental sulfur generation in sulfide and nitrate removal process: characterization, pathway, and microbial community analysis. Appl Microbiol Biotechnol 100:2895–2905. https://doi.org/10.1007/s00253-015-7146-4

Warren LA, Norlund KLI, Bernier L (2008) Microbial thiosulphate reaction arrays: the interactive roles of Fe(III), O_2 and microbial strain on disproportionation and oxidation pathways. Geobiology 6:461–470. https://doi.org/10.1111/j.1472-4669.2008.00173.x

Wasmund K, Mußmann M, Loy A (2017) The life sulfuric: microbial ecology of sulfur cycling in marine sediments. Environ Microbiol Rep 9:323–344. https://doi.org/10.1111/1758-2229.12538

Watanabe T, Kojima H, Umezawa K, Hori C, Takasuka TE, Kato Y, Fukui M (2019) Genomes of neutrophilic sulfur-oxidizing chemolithoautotrophs representing 9 proteobacterial species from 8 genera. Front Microbiol 10:1–13. https://doi.org/10.3389/fmicb.2019.00316

Wei C, Sun D, Yuan W, Li L, Dai C, Chen Z, Zeng X, Wang S, Zhang Y, Jiang S, Wu Z, Liu D, Jiang L, Peng S (2023) Metagenomics revealing molecular profiles of microbial community structure and metabolic capacity in Bamucuo lake. Tibet Environ Res 217:114847. https://doi.org/10.1016/j.envres.2022.114847

Whaley-Martin K, Jessen GL, Colenbrander-Nelson T, Mori JF, Apte SC, Jarolimek C, Warren LA (2019) The potential role of *Halothiobacillus* spp. in sulfur oxidation and acid generation in circum-neutral mine tailings reservoirs. Front Microbiol. https://doi.org/10.3389/fmicb.2019.00297

Whaley-Martin K, Marshall S, Colenbrander-Nelson T, Twible L, Jarolimek CV, King JJ, Apte SC, Warren LA (2020) A mass-balance tool for monitoring potential dissolved sulfur oxidation risks in mining impacted waters. Mine Water Environ 39:291–307. https://doi.org/10.1007/s10230-020-00671-0

Whaley-Martin KJ, Chen L-X, Nelson TC, Gordon JG, Kantor R, Twible LE, Marshall S, McGarry S, Rossi L, Bessette B, Baron C, Apte S, Banfield JF, Warren LA (2023) O_2 partitioning of sulfur oxidizing bacteria drives acidity and thiosulfate distributions in mining waters. Nat Commun 14:2006. https://doi.org/10.1038/s41467-023-37426-8

Wood AP, Woodall CA, Kelly DP (2005) *Halothiobacillus neapolitanus* strain OSWA isolated from "The Old Sulphur Well" at Harrogate (Yorkshire, England). Syst Appl Microbiol 28:746–748. https://doi.org/10.1016/j.syapm.2005.05.013

Xu S, Chen M, Feng T, Zhan L, Zhou L, Yu G (2021) Use ggbreak to effectively utilize plotting space to deal with large datasets and outliers. Front Genet. https://doi.org/10.3389/fgene.2021.774846

Zhang J, Liu R, Xi S, Cai R, Zhang X, Sun C (2020) A novel bacterial thiosulfate oxidation pathway provides a new clue about the formation of zero-valent sulfur in deep sea. ISME J 14:2261–2274. https://doi.org/10.1038/s41396-020-0684-5

Zhang R-C, Xu X-J, Chen C, Shao B, Zhou X, Yuan Y, Lee DJ, Ren NQ (2019) Bioreactor performance and microbial community analysis of autotrophic denitrification under micro-aerobic condition. Sci Total Environ 647:914–922. https://doi.org/10.1016/j.scitotenv.2018.07.389